Effects of Horizontal Vibration on Hopper Flows of Granular Materials

R.C. Weathers[1], M.L. Hunt[2], C.E. Brennen[3], A.T. Lee[4] and C.R. Wassgren[5]

Abstract

This study experimentally examines the flow of glass spheres in a wedge-shaped hopper that is vibrated horizontally. When the hopper is discharged without vibration, discharge occurs as a funnel flow, with the material exiting the central region of the hopper and stagnant material along the sides. With vibration, the discharge of the material occurs in reverse, with the material along the sides exiting first, followed by the material in the central region. These patterns are observed with flow visualization and high-speed photography. The study also includes measurements of the discharge rate, which increases with the amplitude of the velocity of vibration.

Introduction

The discharge of material from a hopper is common practice in many different types of industries (Shamlou, 1988; Nedderman, 1992). The flow patterns and discharge rates are dictated by the geometry and surface conditions of the hopper and the characteristics of the stored material. In general, hoppers are classified in two different types: mass flow and funnel flow. In a mass-flow hopper, all of the material moves as the hopper is discharged; in a funnel-flow design, the movement of the material is confined to the vertical region in the center of the hopper. Hence, for mass flow hoppers, the material that enters the hopper first is discharged first; in a funnel-flow hopper, the material that enters first is discharged last. The inclined walls of the mass flow design must be steep, with the necessary angle dependent on the type of

[1] Undergraduate student, Division of Engineering and Applied Science, Mail Code 104-44, California Institute of Technology, Pasadena, CA, 91125.
[2] Professor, author to whom correspondence should sent.
[3] Professor.
[4] Graduate student, Mechanical Engineering Department, University of California, Berkeley, CA.
[5] Professor, Department of Mechanical Engineering, Clemson University, Clemson, SC.

material involved. To date, the problem of predicting the necessary angle for mass flow, and the resulting discharge rate relies on considerable empirical data (Nguyen, Brennen and Sabersky, 1980; Wieghardt, 1975). However, simple analyses of discharging hopper are able to predict the functional dependence of the discharge rate on the hopper exit width, B (Shamlou, 1988; Nedderman, 1992). From these studies the discharge rate, W, for a planar hopper should vary as follows:

$$W = C\rho g^{1/2} A(B - kd)^{1/2}$$

where ρ is the density of the material, g is the gravitational constant, A is the effective area of the hopper orifice, B is the opening width and d is a particle diameter. The constant, C, is of order unity and depends on the type of material, discharge angle, hopper geometry and surface conditions. The constant, k, is used to correct for the empty space around the edge of the orifice, which cannot be occupied by a solid particle.

To increase the mobility of material within a hopper, a live-wall design is often used in which an out-of-balance motor is attached to the side of the hopper. These motors cause the wall to vibrate in both the vertical and the horizontal directions. The aim is to place the motor in an appropriate position to maintain movement of the material.

The present study examines the effect of horizontal vibration on the discharge of material from a planar hopper. Unlike the live-wall design, the entire hopper is vibrated on a shaker table. The focus is to understand the flow patterns induced by the vibration so that the results might aid in better designs for vibrating hoppers. To date, there appears to be little other work in the area of vibrating hoppers. The recent work by Wassgren (1996) is an exception; this thesis examined the effect of vertical vibration on containers filled with granular material including the discharge from a hopper. The results show that the vertical vibration could both increase or decrease the discharge rate depending on the vibration velocity and acceleration. The effects of horizontal vibration, however, were not included.

Experimental Facility and Method

The experimental planar hopper is shown in Figure 1. The vertical front and back surfaces are double layered, with the inner surface made from 3-mm thick tempered glass and the outer surface of 12.7-mm lucite. The purpose of the inner glass plates is to minimize electrostatic charge and to maximize the flow slippage along the surface. The lucite outer walls provides structural integrity for the hopper. The 45° side walls are smooth-milled lucite surfaces. The depth of the hopper is 1.27 cm and the hopper opening is 1.75 cm. From side wall to side wall the hopper is 29.75 cm, the overall height is 33 cm and the height of the bin above the 45° side walls is 19 cm. A thin metal plate blocks the hopper opening. This plate is withdrawn to initiate the discharge experiments.

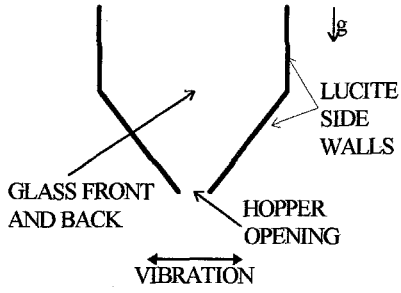

Figure 1. Diagram of horizontal vibrating hopper.

The hopper is mounted on a thick aluminum plate that is attached to the shaker table. The table provides sinusoidal, horizontal vibrations with variable frequency and acceleration. A metal collection bucket is mounted to the aluminum plate below the hopper. The materials used are spherical glass beads of 1 mm or 2 mm diameter. For some flow visualization experiments, the beads were dyed with a water-based paint. The beads and the hopper were periodically washed to minimize the effects of dirt and static electricity.

Using a as the amplitude of the vibration, and ω as the angular frequency, the vibration of the plate can be described in terms of its maximum velocity, $a\omega$, or its acceleration, $a\omega^2$. Similarly, the vibration can also be defined in terms of the Hertzian frequency, $f=2\pi\omega$. The two governing non-dimensional parameters are the acceleration amplitude, $\Gamma=a\omega^2/g$, and the vibration amplitude, $\Omega=a\omega/V_d$ where V_d is a characteristic velocity of discharge, which is taken as $V_d=[g(B-kd)]^{1/2}$.

In the first set of experiments, the discharge rate of the material was measured for both 1 mm and 2 mm beads. The vibrational frequency ranged from 5 to 35 Hz, and accelerations from 0 to a maximum of 3.0 g at the highest frequency. At lower frequencies, the maximum acceleration was limited because of bead loss from the open hopper and limitations of the shaker.

For each experiment, 1.2 kg of material was placed in the hopper. By measuring the mass of the material at the end of the experiment, the bead loss was found to always be less than 1 %. The flow was initiated by manually removing the hopper plug. The discharge rate was timed, and the rate was compared to the discharge rate without vibration measured in an experiment on the same day. Day to day variations occurred due to temperature, humidity and static charge. Each data point presented in the subsequent figures represents an average of 6 measurements. The variations between runs were as much as 10 percent of the average.

Visualization with of the discharging material was done using a standard 30-frames per second CCD camera and with a high-speed (up to 500 frames per second) digital camera.

Discharge Rates

Figures 2 and 3 present the discharge rate, W, with a vibrating hopper divided by the discharge rate without vibration, W_o, for the 1 and 2 mm glass beads. The discharge rates are presented in terms of the non-dimensional acceleration amplitude, Γ. The figures show that the discharge rate increases with vibrational acceleration. However, at the higher frequencies, the increase in discharge rate does not occur until the acceleration amplitude is greater than approximately $\Gamma \approx 1$. The discharge rate also depends on the frequency of vibration, with the lowest frequencies resulting in the highest discharge rates for a fixed acceleration level.

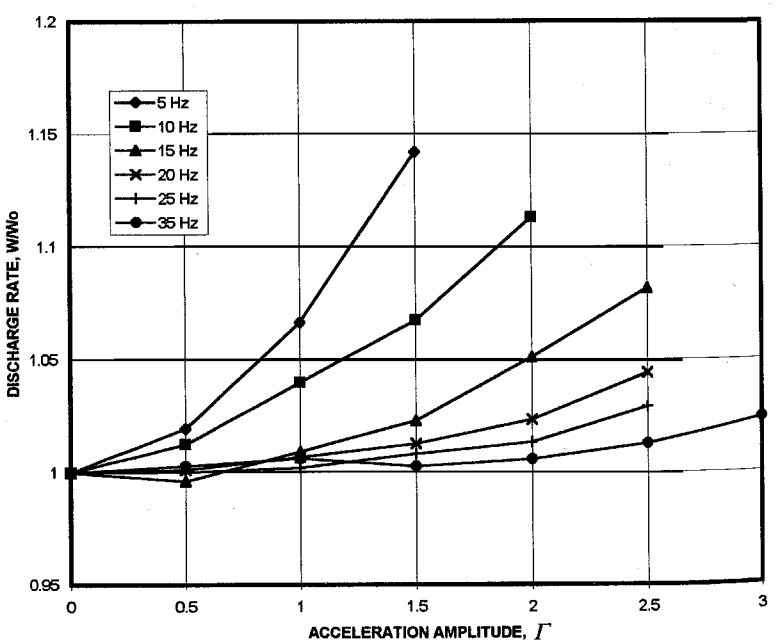

Figure 2. Discharge rate as a function of acceleration amplitude, Γ, for 1-mm spheres.

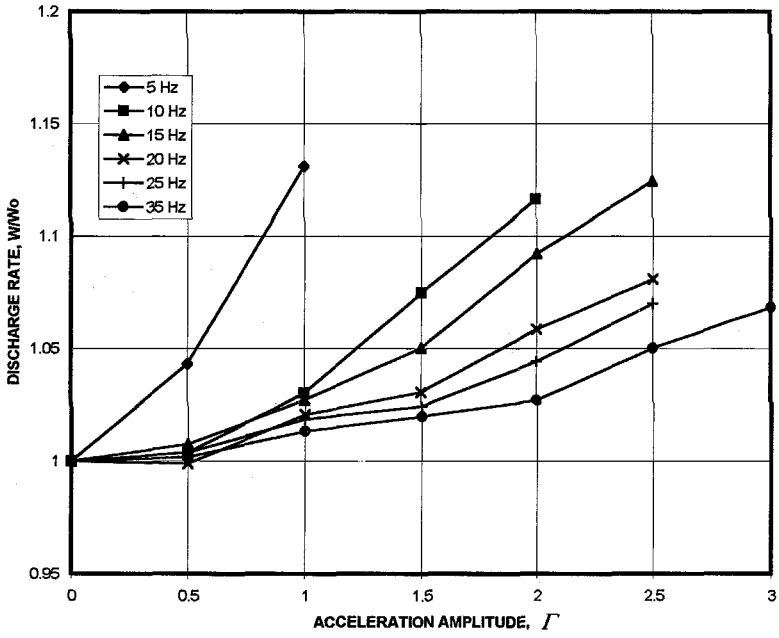

Figure 3. Discharge rate as a function of acceleration amplitude, Γ, for 2-mm spheres.

Figure 4 presents the same discharge results; however, the discharge rate is in terms of the non-dimensional vibrational velocity, Ω. In terms of Ω, the results fall closer together, suggesting that the discharge rate is strongly dependent on the vibrational velocity. For a fixed, Γ, the discharge rate increases with vibrational velocity. The figure also shows that below $\Omega = 0.1$ there is negligible effect of the vibration on the discharge rate. In addition, the difference between the results for the 1-mm and the 2-mm spheres is small. A value of $k=1.5$ is used to define a characteristic velocity of discharge (Nedderman, 1992).

Flow Visualization

The flow was visualized by layering colored and non-colored particles. Figures 5a - 5d show digitized images of the discharging hopper without vibration. Clearly, the material is first discharged from the central region of the hopper. The material then avalanches down the sloped upper surfaces so that the material adjacent to the 45° surfaces discharges last. The upper surface forms an angle of approximately 125°.

Figures 6a - 6d shows the effect of vibration on the flow patterns for a vibration of Γ=2.0 at 20 Hz. In Figure 6a, the hopper is closed and the only visible

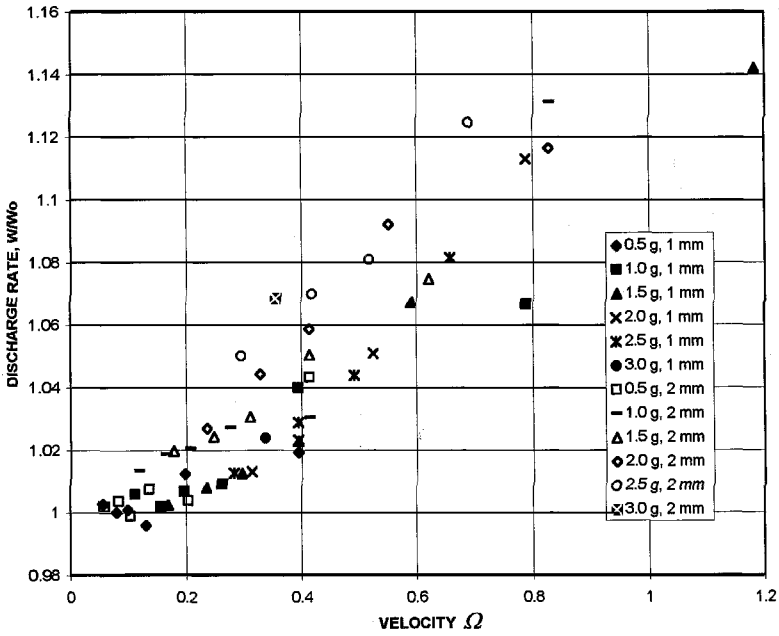

Figure 4. Discharge rates in terms of vibrational velocity, Ω for 1 and 2-mm spheres.

movement of the material occurs in the upper corners of the hopper. Visual observations show that the material moves down along the vertical side walls and then recirculates up through the bed of material. The result of this motion is the triangular mixed region observed in the figure. The mixed region does not increase in size after the initial transient period. Under close inspection, it was observed that a gap opened between the sides of the hopper and the material. Hence, as the hopper is moved in a particular direction, the material within the hopper lags behind, allowing for a small opening. After the hopper reverses direction, the material and the hopper wall reconnect. The depth of the gap appears to extend to the corner between the vertical surface and the sloped surface.

When the hopper is discharged, the flow patterns are almost opposite of those observed without vibration as seen in Figures 6b-6d. The material along the sloped surfaces discharges first, and the material in the central upper region discharges last. After an initial transient period, the upper surface forms an angle of approximately 210°. This angle remains relatively constant throughout the discharge period. The material on the upper free surface avalanches towards the wall.

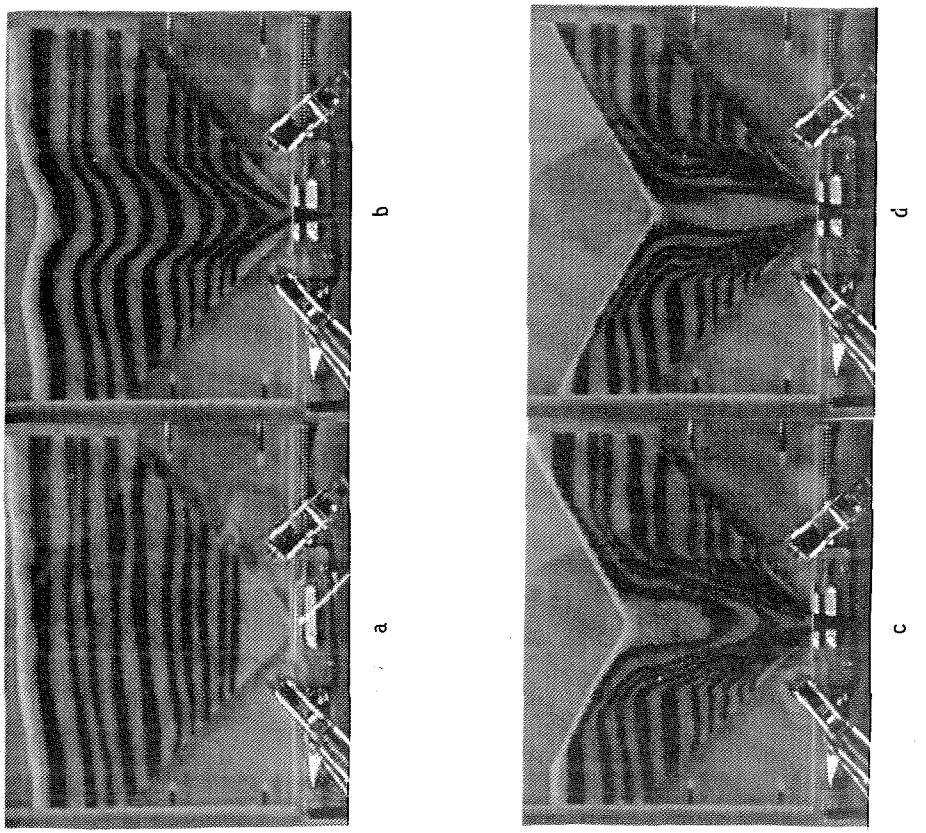

Figure 5. Digitized images of the discharging hopper without vibration. Image 5a is before opening of the hopper. The progression proceeds in 5b, 5c and 5d.

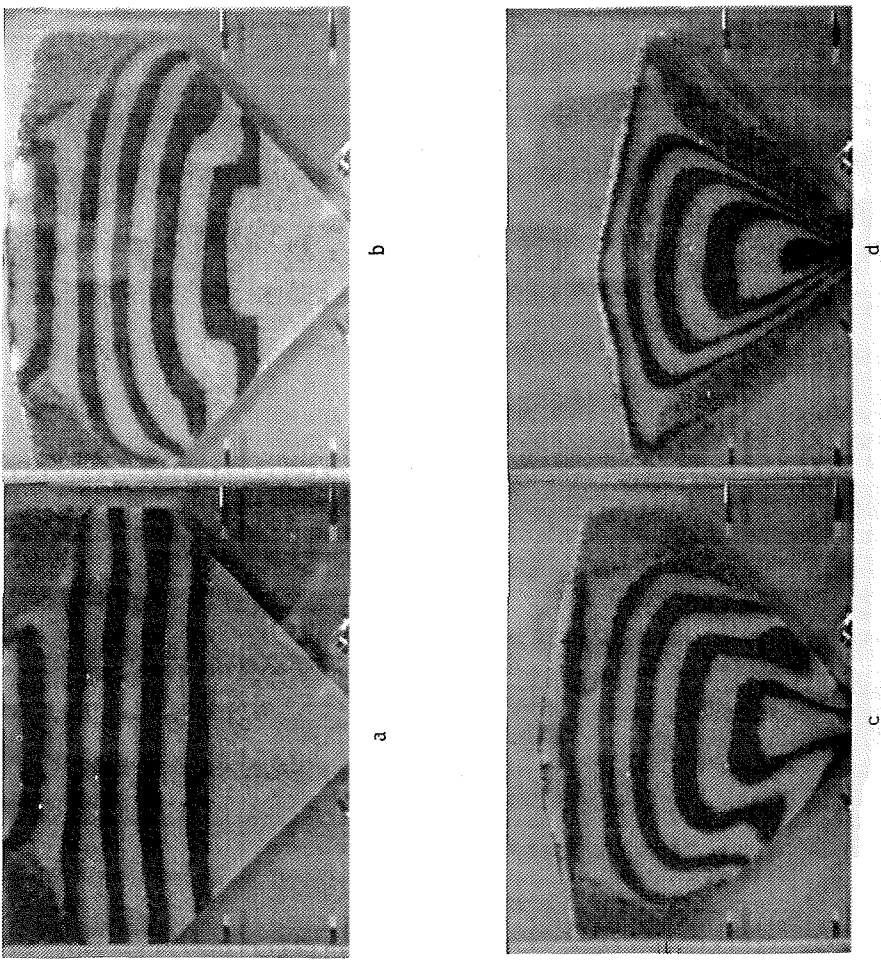

Figure 6. Digitized images of the hopper with horizontal vibration at 20 Hz and 2 *g*. In 5a, the hopper is not opened and circulation is viewed in the upper corner. In 5b, 5c and 5d the hopper is discharging.

By monitoring the material near the side walls with the high-speed camera, it was observed that over most of the vibration cycle, the particles along the side walls moved with the hopper. The short period that the particles are not in synch with the hopper occurs as the hopper reverses directions. Consider the sketch of a particle on an inclined surface shown in Figure 7. The particle may lose contact with the surface as the surface is moved in the x-direction. However, if the surface decelerates (as in the case of a sinusoidal vibration), the particle and the surface will reconnect. This separation and reconnection appears to be what happens during a vibration cycle. As the hopper moves to the right, the particles adjacent to the left inclined surface remain in contact. As the hopper reverses directions moving to the left, the material along this surfaces loses contact and falls under gravity a short distance until it impacts the surface at a position closer to the exit of the hopper. The average downward velocity of the particle can be calculated from the following simple analysis.

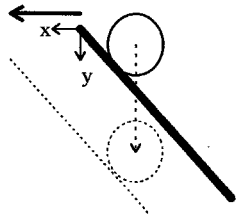

Figure 7. Vertical displacement of a particle due to horizontal motion and subsequent deceleration of the inclined plate.

The movement of the plate in the x-direction is sinusoidal, $x = a\sin(\omega t)$. Hence after some time τ the plate has moved a horizontal distance, $a[1\text{-}\cos(\omega\tau)]$. At time τ, a vertical gap has opened for the particle to fall; this vertical distance is $a[1\text{-}\cos(\omega\tau)]\tan\theta$, where θ is the inclination angle of the plate. If the particle has no initial vertical velocity, the distance that it can fall in time τ, is $g\tau^2/2$. Hence, the particle and the surface will reconnect when

$$g\tau^2 / 2 = a[1 - \cos(\omega\tau)]\tan\theta \qquad (1)$$

Using $a = \Gamma g / \omega^2$, this equation can be rewritten as

$$(\omega\tau)^2 / [1 - \cos(\omega\tau)] = 2\Gamma\tan\theta \qquad (2)$$

which can be solved for the time of flight τ. Figure 8 shows the roots of Equation (2) in terms of $\omega\tau$ as a function of $\Gamma\tan\theta$. The figure shows that there are no solutions to

the equation for $\Gamma\tan\theta<1$. For these conditions, the particle would not separate from the surface. For $\Gamma\tan\theta>1$, $\omega\tau$ increases with acceleration level. The average downward velocity, V, can then be found from the distance traveled during flight divided by the period of oscillation,

$$V = (g\tau^2/2)(\omega/2\pi) = a\omega\tan\theta(1-\cos\omega\tau)/2\pi \quad (3)$$

Hence, if the acceleration level is fixed, $\omega\tau$ is fixed, and the downward velocity depends only on the vibrational velocity, $a\omega$. This observation is observed in Figure 4, which shows that for a fixed Γ that is greater than 1, the discharge rate increases with the vibrational velocity, Ω.

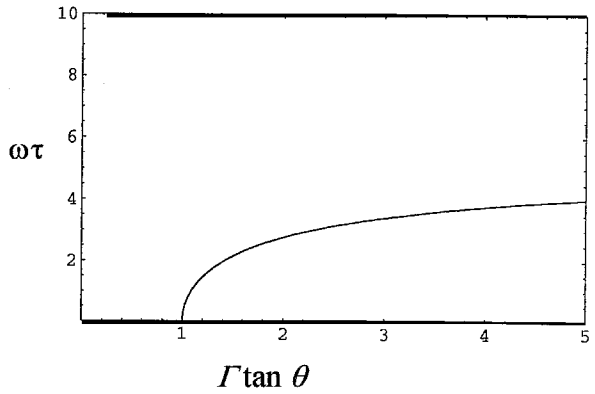

Figure 8. Roots of Equation (2).

Transition from Funnel to Side-Wall Flow

As shown from the visualization in Figures 5 and 6, with no vibration the flow follows a funnel flow pattern; with acceleration at $\Gamma=2.0$, the flow has changed to a side-wall pattern. The transition from one flow type to another occurs over a range of vibrational velocity and acceleration. The change in flow pattern appears to coincide with the increase in the discharge rate. To understand the transition process, the maximum inclination angle of the upper free surface was measured for a hopper vibrating at 35 Hz. The results are presented in Figure 9; clearly the transition occurs over a range of acceleration. However, by $\Gamma\approx1$, the upper surface has reached the maximum angle of inclination.

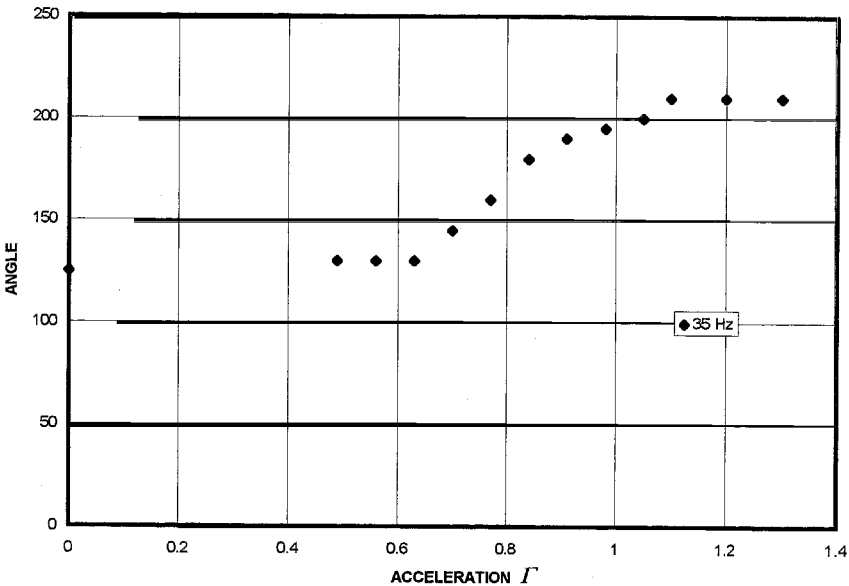

Figure 9. Angle of free surface as a function of acceleration at 35 Hz.

Conclusions

The present work shows that horizontal vibration can increase the discharge rate from a hopper and eliminate the first-in last-out problem that is encountered in funnel-flow designs. For $\Gamma \tan\theta > 1$, the discharge rate increase linearly with vibrational velocity and the flow exhibits a side-wall discharge. For $\Gamma \tan\theta < 1$, the vibration appears to affect the flow pattern only slightly and the flow continues to resemble the funnel-flow pattern observed for no vibration. A simple model suggests that above $\Gamma = 1$ (for $\tan\theta = 1$ in the present case) the particles along the inclined surfaces separate from the surface. The experimental results show that there appears to be a range of vibrational velocity and acceleration in which the flow transitions from one type to another.

The results presented in this paper are part of an ongoing study. Future work will include additional measurements of the local motions of the particles to examine if the simple model presented in this work is able to predict the velocities of the particle along the side walls. In addition, additional studies are also warranted in the determination of the transition process between flow types. An additional aspect of future studies will involve discrete particle simulations which have proven to be a valuable component of granular flow research.

References

Nedderman, R.M., 1992, Statics and Kinematics of Granular Materials, Cambridge University Press.

Nguyen, T.V., Brennen, C.E. and Sabersky, R.H., 1980, ``Funnel Flows in Hoppers", J. Applied Mechanics, 47, 729-735.

Shamlou, P.A., 1988, Handling of Bulk Solids, Theory and Practice, Butterworths, London.

Wassgren, C.R., 1996, Vibration of Granular Materials, Doctoral thesis, California Institute of Technology.

Wieghardt, K., 1975, ``Experiments in Granular Flow," Annual Review Fluid Mechanics, 89-114.